RESEARCH ARTICLE

Neutralizing antibody against osteopontin attenuates non-alcoholic steatohepatitis in mice

Machiko Honda[1] · Chiemi Kimura[2] · Toshimitsu Uede[2] · Shigeyuki Kon[1]

Abstract

Previously, we reported that an extracellular matrix protein, osteopontin (OPN), is involved in various autoimmune diseases using a neutralizing polyclonal antibody against OPN generated in rabbits. However, the antibody cannot be used for long-term mouse models of chronic inflammatory disease because of the induction of antibodies against anti-OPN rabbit IgG. In this study, we generated a new antibody, anti-mouse OPN mouse IgG (35B6). 35B6 inhibited the cell adhesion of mouse and human OPN to Chinese Hamster Ovary (CHO) cells or CHO cells expressing α4 or α9 integrin. It was reported that OPN is highly expressed and has an important role in a chronic liver disease, non-alcoholic steatohepatitis (NASH). 35B6 injection twice a week for 8 weeks attenuated liver inflammation and fibrosis in a NASH mouse model, suggesting 35B6 is beneficial for the treatment of NASH. 35B6 was preferable to the rabbit anti-OPN antibody for investigating the in vivo function of OPN in mouse models of long-term disease.

Abbreviations

CDAHFD	0.1% methionine on a high fat diet background
col1a1	type I collagen α1 chain
CHO	Chinese Hamster Ovary
ECM	extracellular matrix
HE	hematoxylin-eosin
HSC	hepatic stellate cells
RGD	arginine-glycine-aspartate
NAFLD	non-alcoholic fatty liver disease
NASH	non-alcoholic steatohepatitis in mice
OPN	osteopontin
SMA	smooth muscle actin

✉ Shigeyuki Kon
kon@fukuyama-u.ac.jp

Machiko Honda
honda@fukuyama-u.ac.jp

Chiemi Kimura
chiemi@igm.hokudai.ac.jp

Toshimitsu Uede
uedetoshimitsu@gmail.com

[1] Department of Molecular Immunology, Faculty of Pharmaceutical Sciences, Fukuyama University, 985, Sanzo, Higashimura-cho, Fukuyama 729-0292, Japan

[2] Division of Molecular Immunology, Institute for Genetic Medicine, Hokkaido University, Kita-15, Nishi-7, Kita-ku, Sapporo 060-0815, Japan

Introduction

Osteopontin (OPN) is a secreted glycoprotein that mediates cell-matrix interactions and cellular signaling through integrin binding domains including arginine-glycine-aspartate (RGD) motif and SVVYGLR sequences (Yokosaki et al. 1999; Barry et al. 2000a; Denhardt et al. 2001). An important feature of OPN is the presence of a thrombin cleavage site (Denhardt et al. 2001). The non-thrombin cleaved form of OPN binds to RGD motif-recognizing integrins, such as α5β1 and αvβ3 integrins, expressed by various cells, including fibroblasts, endothelial cells, smooth muscle cells, and tumor cells (Barry et al. 2000b; Helluin et al. 2000; Denhardt et al. 2001). In contrast, the thrombin-cleaved form of OPN exposes a cryptic epitope, SVVYGLR, which preferentially binds to α9β1 and α4β1 integrins expressed by leukocytes (Yokosaki et al. 1999; Bayless and Davis 2001; Ito et al. 2009). By binding to these various integrins, OPN induces diverse effects including cell adhesion, migration, immune regulation, angiogenesis, prevention of apoptosis, and tumor

development (Uede et al. 1997; Denhardt et al. 2001; Weber 2001; Mazzali et al. 2002; Rangaswami et al. 2006). Previous studies revealed that OPN is involved in various disease conditions such as multiple sclerosis (Chabas et al. 2001; Shinohara et al. 2008), allergic airway disease (Xanthou et al. 2007; Takahashi et al. 2009), hepatitis (Diao et al. 2004; Kon et al. 2008), and rheumatoid arthritis (Yamamoto et al. 2003; Yamamoto et al. 2007).

To examine OPN functions in vivo, OPN deficient mice, recombinant proteins, or neutralizing antibody can be useful. However, there are several difficulties in using OPN deficient mice and recombinant proteins because the genetic background of mice and endotoxin contamination in recombinant proteins affects OPN functions (Blom et al. 2003; Konno et al. 2005). Therefore, neutralizing antibodies against OPN are a preferable approach to elucidate the functions of OPN. We previously generated a neutralizing antibody against mouse OPN (M5) (Yamamoto et al. 2003; Diao et al. 2004). However, polyclonal M5 antibodies produced in rabbits have the disadvantages of not being applicable for mouse models of disease that require long-term study such as chronic inflammation, because anti-rabbit antibody against M5 emerges. Therefore, additional approaches are needed to analyze OPN functions in vivo. To overcome this problem, we developed a monoclonal antibody (clone 35B6) generated in mice immunized with the VDVPNGRGDSLAYGLR peptide, the peptide used to generate the M5 antibody. The use of 35B6 allows the study of OPN functions in chronic inflammation.

Non-alcoholic steatohepatitis (NASH) is a progressive non-alcoholic fatty liver disease (NAFLD) with an unmet medical need (Chen et al. 2018). The features of NASH include excessive fat accumulation, inflammation, and fibrosis of the liver (Papatheodoridi et al. 2019). OPN is upregulated in the blood and liver of NASH patients as well as NASH mouse models and it is an exacerbation factor of inflammation and fibrosis in NASH models (Sahai et al. 2004; Syn et al. 2011; Coombes et al. 2016). Here, we demonstrate that 35B6 suppresses hepatic inflammation and fibrosis in mice fed a choline-deficient, L-amino acid-defined, high-fat diet (CDAHFD).

Materials and methods

Production of monoclonal antibody against OPN

A synthetic peptide VDVPNGRGDSLAYGLR corresponding to the internal sequence of mouse OPN (Yamamoto et al. 2003; Diao et al. 2004) was coupled with thyroglobulin and used to immunize mice. Spleen cells were harvested and fused with X63-Ag8–653 cells. One clone (35B6; IgG1) was obtained.

Solid-phase binding assay

OPN proteins, synthetic peptides, fibronectin, vitronectin, or laminin (Sigma-Aldrich, St Louis, MO, USA) were coated onto 96-well plates at a concentration of 5 μg/ml at 4 °C overnight, then blocked with 0.1% BSA in PBS containing 0.05% NaN_3 at 37 °C for at least 1 h. The plates were washed twice with PBS and incubated with 35B6 (2 μg/ml) at 37 °C for 1 h. After a further three washes, a 1:5000 dilution of peroxidase conjugated anti-mouse IgG antibody (Jackson ImmunoResearch, Cambridgeshire, UK) was added to each well at room temperature for 30 min. Bound protein was quantified by a colorimetric assay using tetramethylbenzidine as a substrate for 15 min at room temperature. Plates were read at a wavelength of 450 nm.

Cell adhesion assay

The 96-well plates were precoated with human or mouse OPN N-half/GST protein (Ito et al. 2009) (5 μg/ml) at 37 °C for 1 h, followed by treatment with 0.5% BSA in PBS for 1 h at room temperature. Cells in the presence or absence of various concentrations of 35B6 or control antibody (5A1) (Kon et al. 2002) were suspended in DMEM containing 0.25% BSA and 200 μl of a cell suspension (at a cell density of 5×10^4 cells/well) was applied to 96-well plates and incubated for 1 h at 37 °C. The medium was removed from the plates, and all wells were washed twice. Adherent cells were fixed and stained by 0.5% crystal violet in 20% methanol for 30 min. All wells were rinsed three times with water, and adherent cells were then lysed with 20% acetic acid. The resulting supernatants from each well were analyzed by an immunoreader.

Analysis of mRNA expression

Total RNA from livers was extracted by Trizol (Thermo Fisher, Hanover Park, IL, USA). The specific primers used are shown in Table 1. Quantitative real-time PCR analysis of mRNA expression was performed using a LightCycler Fast Start DNA Master SYBR Green I System (Roche Diagnostics, Indianapolis, IN, USA). The expression of mRNA was calculated by LightCycler Software, version 3. Data were standardized to G3PDH.

Elisa

OPN concentrations were measured using ELISA kits according to the manufacturer's instructions (Immuno-Biological Laboratories, Gunma, Japan).

Table 1 Real-time PCR primer sequences

Gene	Sequence of primers
OPN	5′- CCCGGTGAAAGTGACTGATT-3'
	5′- TTCTTCAGAGGACACAGCATTC-3
$\alpha 4$ integrin	5′- TGGAAGCTACTTAGGCTACT-3'
	5′- CTCCCACGACTTCGGTAGTAT-3'
$\alpha 9$ integrin	5′- AAGGCTGCAGCTGTCCCACATGGACGAAG-3'
	5′- TTAGAGAGATATTCTTCACAGCCCCCAAA-3'
α-SMA	5′- CTCTCTTCCAGCCATCTTTCAT-3'
	5′- TATAGGTGGTTTCGTGGATGC-3'
TNF-α	5′- TCTTCTCATTCCTGCTTGTGG-3'
	5′- GGTCTGGGCCATAGAACTGA-3'
Col1a1	5′- CTCCTGGCAAGAATGGAGAT-3'
	5′- AATCCACGAGCACCCTGA-3'
G3PDH	5'-ACCACAGTCCATGCCATCAC-3'
	5'-TCCACCACCCTGTTGCTGTA-3'

Ethical approval

Mice were provided food and water ad libitum. Every effort was made to minimize suffering during injections, and all surgery was performed on humanely sacrificed animals. All animal experiments were performed in accordance with the guidelines of the Bioscience Committee of Fukuyama University and were approved by the Animal Care and Use Committee of Fukuyama University.

Anti-OPN antibody concentration in blood

M5 antibody or 35B6 (300 μg/mice) were intraperitoneally injected into mice every 7 days for 4 weeks and serum was collected on days 1, 3 and 6 after antibody injection. Antibody concentration was calculated by a solid-phase binding assay. Serum collected after antibody treatment was added to immunogen peptide (VDVPNGRGDSLAYGLR peptide)-coated 96-well plates. After 1 h incubation, peroxidase conjugated anti-mouse IgG antibody for 35B6 or M5 antibody was added as described above. Purified M5 antibody or 35B6 was used as a standard.

Concanavalin A-induced hepatitis model

C57BL/6 mice were injected intravenously with 10 mg concanavalin A (ConA) (Sigma-Aldrich) per kilogram of body weight, dissolved in pyrogen-free PBS. M5 or 35B6 (400 μg) was intraperitoneally administered to mice 15 h before ConA challenge. After 24 h, blood samples were collected for ALT and livers were removed for HE staining. The plasma ALT levels were measured by using a standard clinical autoanalyzer (DRICHEM 5500 V; Fujifilm, Tokyo, Japan). Necrotic areas were measured in each section by using ImageJ Software (version 1.52; National Institutes of Health). Necrotic areas were measured in a double-

blind manner. For each tissue, data were obtained using six high power fields (×100).

NASH model

Seven-week-old male C57BL/6 mice were divided into two groups. One group was fed a choline deficient diet supplemented with 0.1% methionine on a high fat diet background (CDAHFD) (A06071302, Research Diets, New Brunswick, NJ, USA) for 8 weeks. The second group was fed a CDAHFD and intraperitoneally injected with 35B6 twice a week for 8 weeks. After 8 weeks, blood samples were collected for ALT and OPN ELISA, and livers were removed for HE and Sirius-red staining. Collagen content was quantified using ImageJ Software by assessment of the area of liver tissue that was stained positively by Sirius-red. For each tissue, data were obtained using six high power fields (×100). The areas were quantified in a double-blind manner. The expression of collagen I was assessed by anti-collagen I antibody ab34710 (Abcam, Cambridge, MA, USA). Sections of paraffin-embedded liver tissues were processed for immunohistochemistry according to the manufacturer's instructions.

Evaluation of the extent of resultant NASH was scored using scaling scores (Brunt et al. 1999). Briefly, steatosis was graded according to the following scale: 0 = normal; 1 = < 33% affected hepatocytes; 2 = 33%–66% affected hepatocytes; and 3 => 66% affected hepatocytes. Ballooning was graded a score of 0–3 based on severity: 0 = none; 1 = rare or few; 2 = moderate; and 3 = many. Lobular inflammation was graded a score of 0–3 based on inflammatory foci per ×20 field: 0 = none; 1 = 2 foci; 2 = 7 foci; and 3 => 4 foci/×20 field.

Western blot analysis

Livers were homogenized in a lysis buffer (50 mM Tris-HCl (pH 7.4), 150 mM NaCl, 1% Triton X-100, and 1× Complete Mini protease inhibitor mixture (Roche Diagnostics). Lysates were fractionated by SDS-PAGE and transferred to a polyvinylidene difluoride membrane (Merck Millipore, Billerica, MA, USA). The filters were then immunoblotted with anti-OPN antibody (O-17), (34E3) (Immuno-Biological Laboratories), or anti-β-actin (Wako, Osaka, Japan). Immunoreactive proteins were visualized using an ECL detection system (PerkinElmer, Boston, MA, USA).

Statistical analysis

Data are presented as the mean ± SEM and are representative of at least three independent experiments. The statistical significance of differences between groups was calculated using a two-tailed Student's *t* test or nonparametric Wilcoxon Mann–Whitney *U*-test where applicable. Differences were

considered significant when *P* was less than 0.05 (*) or 0.005 (**).

Results

Generation and characterization of 35B6

We generated a monoclonal antibody (35B6) by immunizing mice with the VDVPNGRGDSLAYGLR peptide, the same peptide used to generate the M5 antibody previously. To characterize the 35B6 epitope, we tested it within the VDVPNGRGDSLAYGLR antigen peptide. The peptides used in this study are shown in Fig. 1A. Epitope mapping revealed that 35B6 preferentially bound to the GDSLAYGLR peptide in a solid-phase binding assay (Fig. 1B). Because the antigen peptide contains RGD, a common integrin-binding sequence of extracellular matrix proteins (ECMs), we investigated the binding ability of 35B6 to RGD-sequence containing ECMs and found that 35B6 did not recognize fibronectin, vitronectin or laminin (Fig. 1C). Of note, 35B6 recognized mouse and human OPN.

Identification of a mouse α4β1 and α9β1 integrin-binding sequence

The SLAYGLR amino acid sequence was reported to be involved in binding to α4β1 and α9β1 integrins (Yamamoto et al. 2003; Uede 2011). However, it is unknown whether the SLAYGLR sequence has binding ability. Therefore, we examined whether the SLAYGLR peptide bound to α4β1 and α9β1 integrins using a cell adhesion test with CHO cells expressing mouse α4 integrin or mouse α9 integrin (Kanayama et al. 2009; Kouro et al. 2014), because CHO cells express RGD-recognizing integrins but not α4 or α9 integrins (Ito et al. 2009). The SLAYGLR sequence showed weak binding ability for α4β1, but not α9β1, integrin. The GDSLAYGLR sequence, an epitope of 35B6, exhibited significant binding to α9β1 and α4β1 integrins (Fig. 2), indicating the SLAYGLR sequence is not long enough for α4β1 and α9β1 integrin binding, and that the GDSLAYGLR sequence is the binding sequence for α4β1 and α9β1 integrins.

35B6 Inhibits cell RGD, α4β1 and α9β1 integrin-dependent cell adhesion to mouse and human OPN

We examined whether 35B6 had an inhibitory function using a cell adhesion test. We used the amino-terminal half of OPN (OPN N half) because it was shown to be a ligand of RGD-recognizing α4β1 and α9β1 integrins (Yokosaki et al. 1999; Barry et al. 2000a; Ito et al. 2009). CHO cells or CHO cells expressing mouse α4 integrin or mouse α9 integrin were used when mouse OPN was used as a coating protein, and CHO cells or CHO cells expressing human α4 integrin or human α9 integrin (Ito et al. 2009) were used when human OPN was
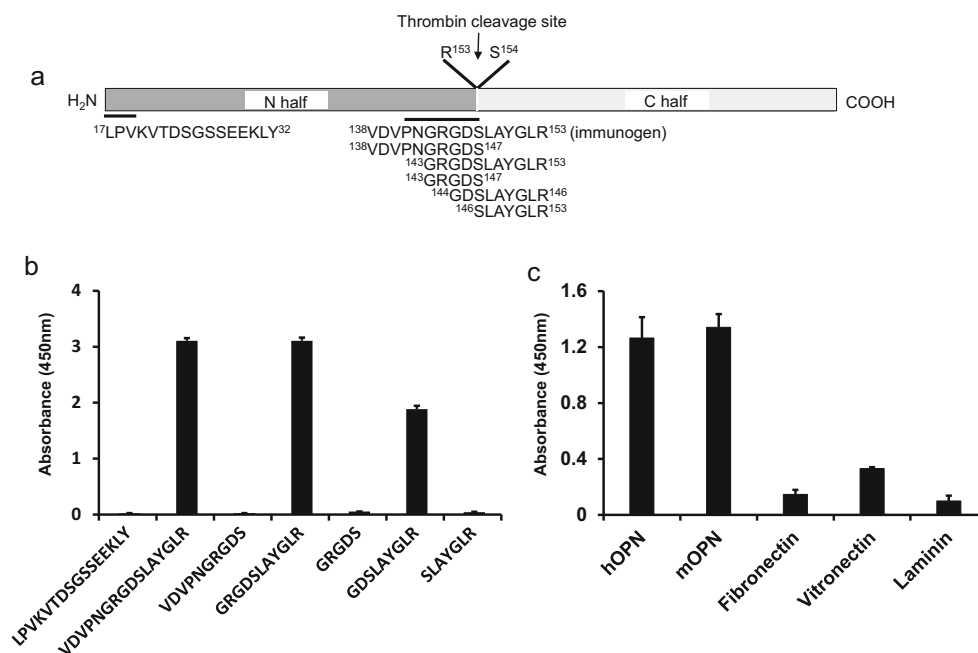

Fig. 1 Characterization of mAb 35B6. A. Mouse OPN structure and synthetic peptide. The position of the thrombin cleavage site (between R^{153} and R^{154}) and seven peptide sequences used for solid-phase binding assay are indicated. B-C. The synthetic peptides (5 μg/ml) (B), human OPN (hOPN), mouse OPN (mOPN), or fibronectin and vitronectin (5 μg/ml) (C) were coated onto 96-well plates. 35B6 at 2 μg/ml was added to protein-coated 96-well plates and the bound antibody was quantified as described in the Materials and Methods. Data are expressed as the mean of triplicate experiments
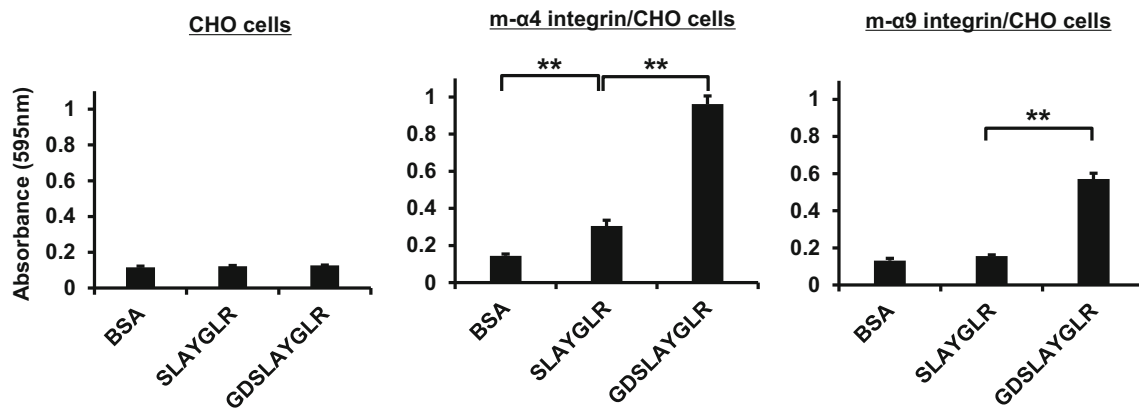
Fig. 2 Identification of mouse $\alpha4\beta1$ and $\alpha9\beta1$ integrin-binding sequences. Cell adhesion test results using BSA, SLAYGLR, or GDSLAYGLR peptides (5 μg/ml) with CHO cells or CHO cells expressing mouse $\alpha4$ or $\alpha9$ integrins. Data are presented as means ± SEM. *, $P < 0.05$; **, $P < 0.005$

used. 35B6 successfully inhibited the cell adhesion of mouse and human OPN to CHO cells or CHO cells expressing $\alpha4$ or $\alpha9$ integrin (Fig. 3A and B). 35B6 did not affect cell adhesion on the irrelevant substrates, fibronectin and vitronectin (Fig. 3C), indicating that 35B6 specifically inhibits OPN function. Cell adhesion inhibitory analysis revealed that 35B6 inhibited RGD-dependent cell adhesion as well as $\alpha4\beta1$ and $\alpha9\beta1$ integrin-dependent cell adhesion, although the epitope of

35B6 was GDSLAYGLR not GRGDS. This may be caused by steric hindrance because the GRGDS sequence is adjacent to the $\alpha4\beta1$ and $\alpha9\beta1$ integrin-binding sites.

To confirm that 35B6 persisted in the blood, we injected M5 or 35B6 into mice once a week and monitored the serum concentration of each antibody. 35B6 remained in the blood for at least 4 weeks, whereas the M5 antibody did not increase in concentration after the third injection
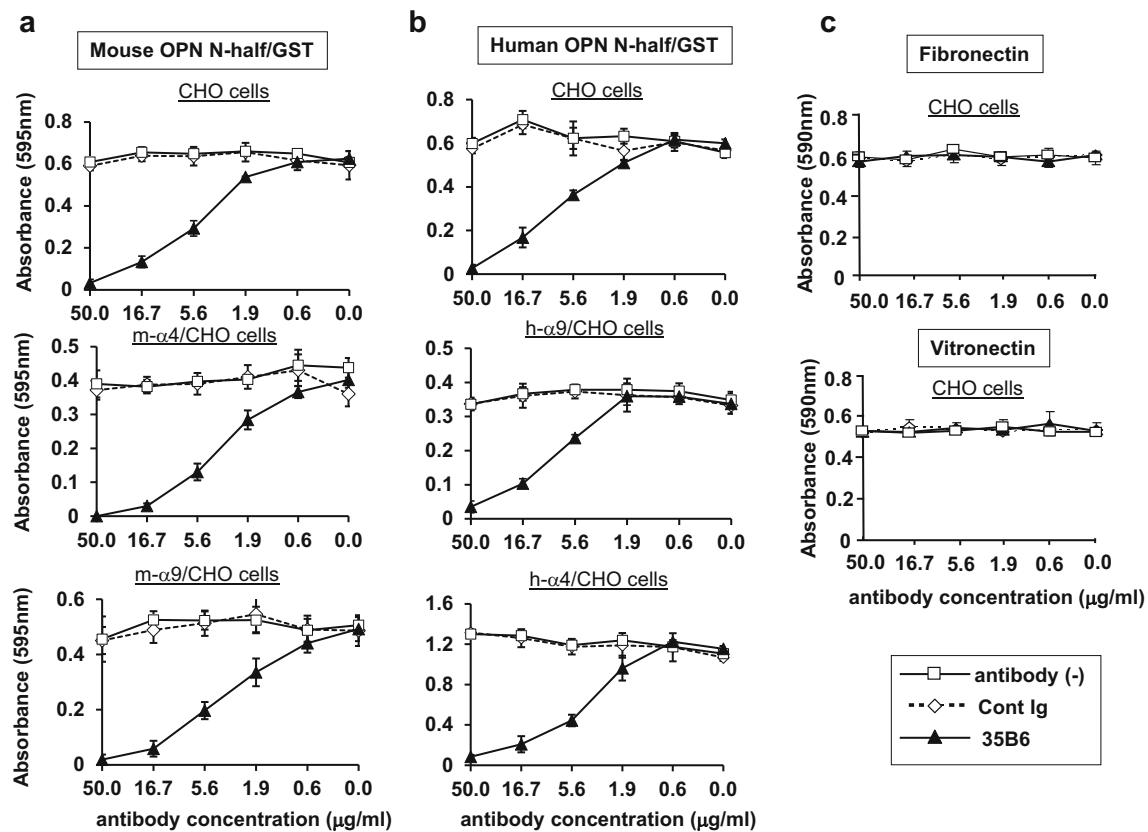

Fig. 3 35B6 inhibits the binding of OPN to CHO cells expressing integrin receptors. The inhibitory effects of 35B6 were assessed by cell adhesion assay. Cell adhesion inhibitory effect of 35B6 for mouse OPN (A), human OPN (B), or fibronectin and vitronectin (C) with CHO cells or CHO cells expressing $\alpha4$ or $\alpha9$ integrins

(Fig. 4), indicating that 35B6 can be used to inhibit OPN in long-term studies.

35B6 Inhibits ConA-induced hepatic injury

To confirm 35B6 has inhibitory effects on OPN function in vivo, we investigated whether 35B6 inhibited ConA-induced hepatitis because we previously reported that M5 protected mice from ConA-induced hepatitis (Diao et al. 2004). 35B6 treatment significantly ameliorated ConA-induced hepatitis as determined by the level of plasma ALT (Fig. 5A) and liver histology (Fig. 5B, C). The inhibitory effect of 35B6 was comparable with M5. Thus, 35B6 can be used to evaluate the in vivo function of OPN.

35B6 Inhibits the infiltration of inflammatory cells and fibrosis in NASH livers

A characteristic of NASH is the presence of hepatic inflammation and continued inflammation in the liver is thought to drive the development of fibrosis. It was reported that OPN is upregulated in the blood and liver and is involved in hepatic inflammation and fibrosis in NASH (Sahai et al. 2004; Syn et al. 2011; Coombes et al. 2016). However, whether NASH can be inhibited by blocking OPN function with an antibody is unknown. Therefore, we investigated whether 35B6 affected NASH progression in mice. To induce NASH, a CDAHFD was fed to mice for 8 weeks. Before antibody treatment, we analyzed OPN expression in NASH livers. OPN mRNA tended to be increased in livers ($P = 0.052$) by real-time PCR and OPN production was significantly upregulated in the liver by ELISA (Fig. 6A). Upregulated OPN expression was re-confirmed by western blotting (Fig. 6B). Of note, thrombin-cleaved OPN was detected by western blotting using antibody against thrombin-cleaved OPN. We next evaluated the expressions of $\alpha 9\beta 1$ and $\alpha 4\beta 1$ integrins because
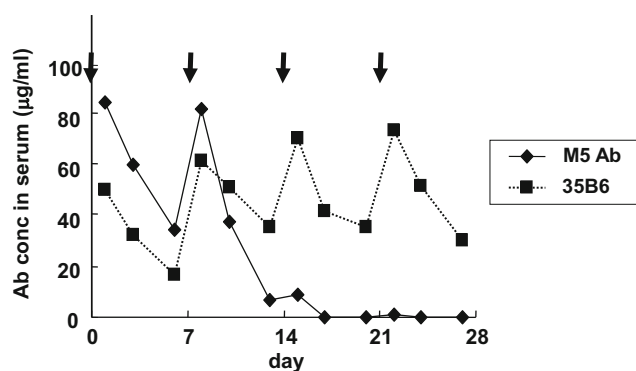
thrombin-cleaved OPN binds to $\alpha 4$ and $\alpha 9$ integrins. Real-time PCR revealed that $\alpha 4$ integrin was significantly upregulated and $\alpha 9$ integrin tended to be increased ($P = 0.096$) in NASH livers (Fig. 6C).

To analyze the effect of 35B6 in NASH progression, 35B6 was injected twice a week during CDAHFD feeding (8 weeks) (Fig. 7A). There was no difference in body weight between control NASH and 35B6-treated mice (Fig. 7B). Plasma ALT levels in 35B6-treated mice tended to be lower than in control NASH mice ($P = 0.12$) (Fig. 7C). Histochemical staining, and HE staining and Sirius-red staining, of NASH livers demonstrated that 35B6 treatment attenuated the infiltration of inflammatory cells and fibrosis, respectively (Fig. 7D, G), whereas there were no obvious differences in the degree of steatosis and ballooning between control NASH and 35B6-treated mice (Fig. 7E, F). Attenuation of fibrosis in 35B6-treated mice was confirmed by immuno-histochemical analysis using anti-collagen I antibody (Fig. 7D). Collagen content was quantified as the percentages of Sirius red-positive areas and we found that 35B6 significantly reduced the degree of liver fibrosis compared with control NASH mice (Fig. 7H). Furthermore, expression of the type I collagen $\alpha 1$ chain (col1a1) analyzed by real-time PCR was significantly decreased in 35B6-treated mice compared with control NASH mice (Fig. 7I). Finally, we analyzed the mRNA expressions of TNF-α and α-SMA, which are inflammation or fibrogenic mediators, respectively. TNF-α and α-SMA mRNA expressions were significantly decreased in the livers of 35B6-treated mice, compared with control NASH (Fig. 7J).

Discussion

There have been many reports of the pathological roles of OPN in inflammatory disease, fibrosis, or tumor development, using OPN deficient mice. However, the genetic background of deficient mice affects the development of various disease models especially immune diseases including collagen-induced arthritis or experimental autoimmune encephalitis (Blom et al. 2003). Therefore, the use of a neutralizing antibody is a preferable approach to analyze the function of OPN in vivo. To date, two neutralizing antibodies against mouse OPN have been reported: AF-808 antibody by R&D Systems (Xanthou et al. 2007; Murugaiyan et al. 2008) and M5 (Yamamoto et al. 2003; Diao et al. 2004). However, these polyclonal antibodies are generated in goats (AF-808) or rabbits (M5) and do not persist in the blood to inhibit OPN function over long periods because an anti-idiotype antibody against anti-OPN polyclonal antibody is induced. Indeed, Fig. 4 indicates that the antibody concentration of M5 was maintained for only 2 weeks in mice. In this study, we generated a mouse monoclonal antibody in mice and confirmed

Fig. 4 Antibody concentration in serum after anti-OPN antibody injection. M5 antibody or 35B6 (300 μg/mice) were injected into mice every 7 days for 4 weeks. Arrows indicate antibody injection days. Sera were collected on days 1, 3 and 6 after antibody injection. Antibody concentration was tested by a solid-phase binding assay using an immunogen-coated plate coated with antigen peptide

Fig. 5 Inhibitory effect of M5 and 35B6 on the development of ConA-induced hepatitis. C57BL/6 mice were intraperitoneally treated with M5 or 35B6 antibody (400 μg/head) at 15 h before ConA injection. Plasma ALT levels (A) and HE staining (B) at 24 h after ConA injection are shown. Dotted line denotes necrotic area. Necrotic areas per liver section were quantified by ImageJ software. Data are presented as means ± SEM. *, $P < 0.05$; **, $P < 0.005$. Bar = 100 μm
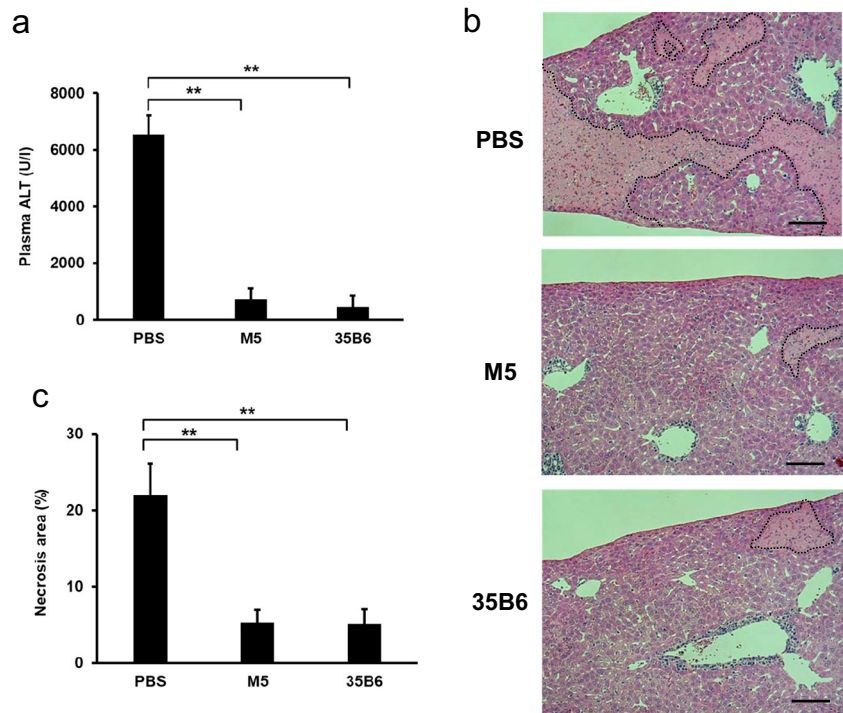
that the antibody titer of 35B6 in the blood was maintained for at least 1 month by treatment once a week. Furthermore, 35B6 recognized human OPN and inhibited the binding of mouse and human OPN to OPN receptors, and RGD-recognizing α4 and α9 integrins, indicating it

might help elucidate the role of OPN in the pathogenesis of disease in humans and various animal models.

Non-alcoholic fatty liver disease (NAFLD) is the most common chronic liver disease, and some patients (approximately 10%–20%) develop NASH, which has a high risk for
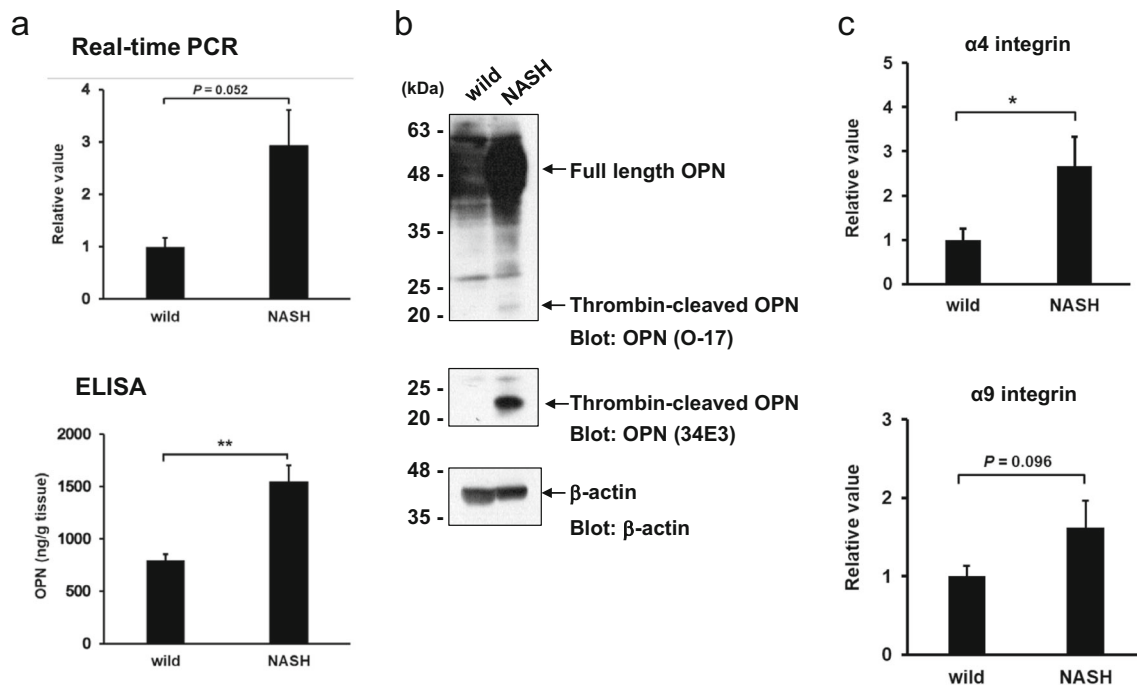

Fig. 6 Expression of OPN in NASH livers. A. Expression of OPN in NASH analyzed by real-time PCR (upper panel) and ELISA (lower panel). B. Expression of OPN and thrombin-cleaved OPN in NASH by western blotting. C. Expression of α4 (upper panel) or α9 integrins (lower panel) in NASH analyzed by real-time PCR. Data are presented as means ± SEM. *, $P < 0.05$; **, $P < 0.005$

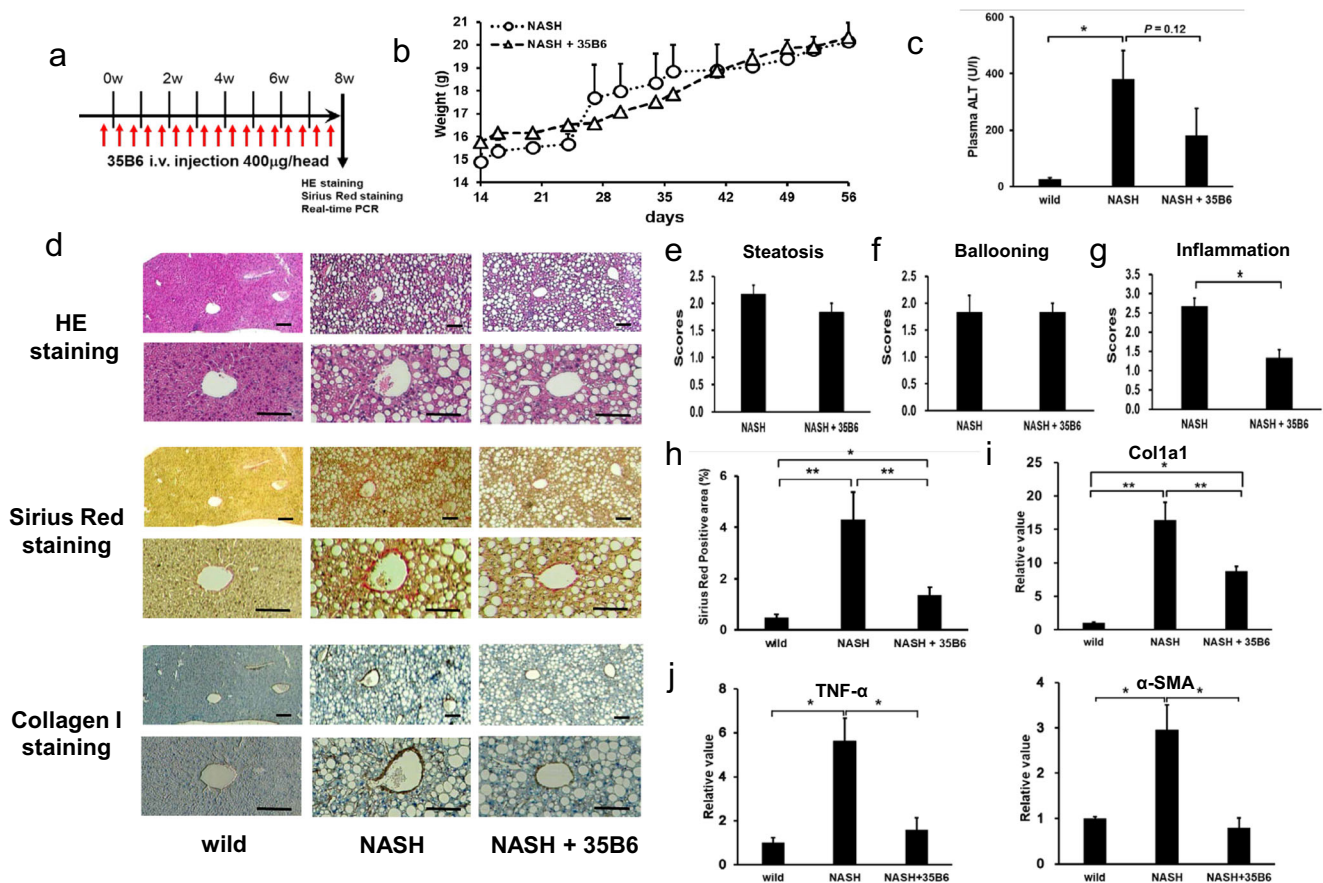**Fig. 7** 35B6 protects mice from NASH progression. A. Protocol for NASH with anti-35B6 treatment. B. Change in body weight. C. Plasma ALT levels at 8 weeks after feeding with CDAHFD. D. Representative liver histology of mice treated with 35B6, control NASH mice, or wildtype mice. Livers were obtained at 8 weeks after feeding with CDAHFD and 35B6 treatment. Liver sections were stained with HE, Sirius Red, or anti-collagen I antibody. Original magnification, ×40 (upper panel) or ×100 (lower panel). Scale bar = 100 μm. E. Scale scores of steatosis (E), ballooning (F) and inflammation (G). H. Quantification of Sirius Red stained images by ImageJ software. Relative mRNA expression levels of col1a1 and col3a1 (I), and TNF-α and α-SMA (J) analyzed by real-time PCR in livers obtained after 8 weeks of treatment. Data are presented as means ± SEM. *, $P < 0.05$; **, $P < 0.005$

cirrhosis or hepatocellular carcinoma (Chen et al. 2018; Papatheodoridi et al. 2019). CDAHFD feeding in mice is a well-established NASH model with similar histological features to human NASH patients including hepatic inflammation and pericellular fibrosis (Matsumoto et al. 2013). It was reported that OPN levels were upregulated in the liver tissues and blood of NASH patients and in NASH mouse models (Sahai et al. 2004). Furthermore, the loss of OPN function reduced liver inflammation and fibrosis in mouse models of NASH (Syn et al. 2011; Coombes et al. 2016). In this study, we confirmed the reduction of inflammation and fibrosis in NASH livers using 35B6. These results implicate RGD-recognizing integrins such as αvβ3, α4, or α9 in NASH progression, which is an hypothesis requiring specific testing in blocking the relevant integrins. αvβ3 integrin is expressed on hepatic stellate cells (HSC) and is involved in the activation of HSC (Li et al. 2015), and has important proinflammatory functions such as inducing the production of proinflammatory cytokines and activation of leukocytes at sites of inflammation

(Kahles et al. 2014). α4β1 and α9β1 integrins are expressed on neutrophils and macrophages (Uede 2011). Neutrophils generate reactive oxygen species (ROS) that cause lipid peroxidation and HSC migration; thus facilitating cellular injury and fibrosis (Casini et al. 1997). Macrophages produce a variety of cytokines such as TNF-α and TGF-β. Livers contain many natural killer T (NKT) cells. We previously reported that NKT cells express α4β1 and α9β1 integrins (Diao et al. 2004). In that report, OPN secreted from NKT cells augmented NKT cell activation and M5 antibody suppressed concanavalin A (Con A)-induced hepatitis. NKT cells were reported to accumulate and promote fibrosis progression in NASH (Syn et al. 2010).

35B6 treatment showed a partial inhibition of inflammation and fibrosis in NASH livers, which might be associated with the involvement of other integrin ligands in the integrin family. Further studies will be directed at understanding the mechanism by which interactions between integrins and integrin ligands including OPN affect NASH progression.

In this study, 35B6 suppressed hepatic inflammation and fibrosis in mice fed a CDAHFD. However, our study had some limitations. It was reported that a choline deficient diet model, such as the MCD model, does not reflect human NASH pathogenesis (Li et al. 2018) where the metabolic context is distinct between a choline deficient diet model and human NASH. Therefore, further investigations are required to elucidate the role of OPN in NASH pathogenesis by using clinically relevant models such as the high-fat-fed, streptozotocin-induced model (Fujii et al. 2013).

In conclusion, we generated an anti-mouse OPN mouse monoclonal antibody, 35B6, which recognizes mouse and human OPN and blocks the adhesion of human and mouse OPN to OPN receptors. Moreover, 35B6 concentrations were maintained at high levels over a long duration by repeated antibody injection. Thus, 35B6 is a powerful experimental tool to clarify OPN function in the development of various diseases. In this study, we showed that 35B6 treatment suppressed inflammatory cell infiltration and fibrosis in a mouse model of NASH. Therefore, 35B6 might be a useful antibody for the prevention and treatment of hepatic inflammation and fibrosis in NASH.

Author contributions TU and SK designed the study. MH, CK, and SK performed the experiments. SK wrote the manuscript. All authors read and approved the final manuscript.

Compliance with ethical standards

Conflict of interest The authors declare that they have no conflict of interest.

References

Barry ST, Ludbrook SB, Murrison E, Horgan CM (2000a) Analysis of the alpha4beta1 integrin-osteopontin interaction. Exp Cell Res 258: 342–351

Barry ST, Ludbrook SB, Murrison E, Horgan CM (2000b) A regulated interaction between alpha5beta1 integrin and osteopontin. Biochem Biophys Res Commun 267:764–769

Bayless KJ, Davis GE (2001) Identification of dual alpha 4beta1 integrin binding sites within a 38 amino acid domain in the N-terminal thrombin fragment of human osteopontin. J Biol Chem 276: 13483–13489

Blom T, Franzen A, Heinegard D, Holmdahl R (2003) Comment on "the influence of the proinflammatory cytokine, osteopontin, on autoimmune demyelinating disease". Science 299:1845 author reply 1845

Brunt EM, Janney CG, Di Bisceglie AM, Neuschwander-Tetri BA, Bacon BR (1999) Nonalcoholic steatohepatitis: a proposal for grading and staging the histological lesions. Am J Gastroenterol 94: 2467–2474

Casini A, Ceni E, Salzano R, Biondi P, Parola M, Galli A, Foschi M, Caligiuri A, Pinzani M, Surrenti C (1997) Neutrophil-derived superoxide anion induces lipid peroxidation and stimulates collagen synthesis in human hepatic stellate cells: role of nitric oxide. Hepatology 25:361–367

Chabas D, Baranzini SE, Mitchell D, Bernard CC, Rittling SR, Denhardt DT, Sobel RA, Lock C, Karpuj M, Pedotti R, Heller R, Oksenberg JR, Steinman L (2001) The influence of the proinflammatory cytokine, osteopontin, on autoimmune demyelinating disease. Science 294:1731–1735

Chen W, Zhang J, Fan HN, Zhu JS (2018) Function and therapeutic advances of chemokine and its receptor in nonalcoholic fatty liver disease. Ther Adv Gastroenterol 11:1756284818815184

Coombes JD, Choi SS, Swiderska-Syn M, Manka P, Reid DT, Palma E, Briones-Orta MA, Xie G, Younis R, Kitamura N, Della Peruta M, Bitencourt S, Dolle L, Oo YH, Mi Z, Kuo PC, Williams R, Chokshi S, Canbay A, Claridge LC, Eksteen B, Diehl AM, Syn WK (2016) Osteopontin is a proximal effector of leptin-mediated non-alcoholic steatohepatitis (NASH) fibrosis. Biochim Biophys Acta 1862:135–144

Denhardt DT, Noda M, O'Regan AW, Pavlin D, Berman JS (2001) Osteopontin as a means to cope with environmental insults: regulation of inflammation, tissue remodeling, and cell survival. J Clin Invest 107:1055–1061

Diao H, Kon S, Iwabuchi K, Kimura C, Morimoto J, Ito D, Segawa T, Maeda M, Hamuro J, Nakayama T, Taniguchi M, Yagita H, Van Kaer L, Onoe K, Denhardt D, Rittling S, Uede T (2004) Osteopontin as a mediator of NKT cell function in T cell-mediated liver diseases. Immunity 21:539–550

Fujii M, Shibazaki Y, Wakamatsu K, Honda Y, Kawauchi Y, Suzuki K, Arumugam S, Watanabe K, Ichida T, Asakura H, Yoneyama H (2013) A murine model for non-alcoholic steatohepatitis showing evidence of association between diabetes and hepatocellular carcinoma. Med Mol Morphol 46:141–152

Helluin O, Chan C, Vilaire G, Mousa S, DeGrado WF, Bennett JS (2000) The activation state of alphavbeta 3 regulates platelet and lymphocyte adhesion to intact and thrombin-cleaved osteopontin. J Biol Chem 275:18337–18343

Ito K, Kon S, Nakayama Y, Kurotaki D, Saito Y, Kanayama M, Kimura C, Diao H, Morimoto J, Matsui Y, Uede T (2009) The differential amino acid requirement within osteopontin in alpha4 and alpha9 integrin-mediated cell binding and migration. Matrix Biol 28:11–19

Kahles F, Findeisen HM, Bruemmer D (2014) Osteopontin: a novel regulator at the cross roads of inflammation, obesity and diabetes. Molecular metabolism 3:384–393

Kanayama M, Kurotaki D, Morimoto J, Asano T, Matsui Y, Nakayama Y, Saito Y, Ito K, Kimura C, Iwasaki N, Suzuki K, Harada T, Li HM, Uehara J, Miyazaki T, Minami A, Kon S, UedeT (2009) Alpha9 integrin and its ligands constitute critical joint microenvironments for development of autoimmune arthritis. J Immunol 182:8015–8025

Kon S, Ikesue M, Kimura C, Aoki M, Nakayama Y, Saito Y, Kurotaki D, Diao H, Matsui Y, Segawa T, Maeda M, Kojima T, Uede T (2008) Syndecan-4 protects against osteopontin-mediated acute hepatic injury by masking functional domains of osteopontin. J Exp Med 205: 25–33

Kon S, Yokosaki Y, Maeda M, Segawa T, Horikoshi Y, Tsukagoshi H, Rashid MM, Morimoto J, Inobe M, Shijubo N, Chambers AF, Uede T (2002) Mapping of functional epitopes of osteopontin by

monoclonal antibodies raised against defined internal sequences. J Cell Biochem 84:420–432

Konno S, Hoshi T, Taira T, Plunkett B, Huang SK (2005) Endotoxin contamination contributes to the in vitro cytokine-inducing activity of osteopontin preparations. J Interferon Cytokine Res 25:277–282

Kouro H, Kon S, Matsumoto N, Miyashita T, Kakuchi A, Ashitomi D, Saitoh K, Nakatsuru T, Togi S, Muromoto R, Matsuda T (2014) The novel alpha4B murine alpha4 integrin protein splicing variant inhibits alpha4 protein-dependent cell adhesion. J Biol Chem 289: 16389–16398

Li D, He L, Guo H, Chen H, Shan H (2015) Targeting activated hepatic stellate cells (aHSCs) for liver fibrosis imaging. EJNMMI Res 5:71

Li H, Toth E, Cherrington NJ (2018) Asking the right questions with animal models: methionine- and choline-deficient model in predicting adverse drug reactions in human NASH. Toxicol Sci 161:23–33

Matsumoto M, Hada N, Sakamaki Y, Uno A, Shiga T, Tanaka C, Ito T, Katsume A, Sudoh M (2013) An improved mouse model that rapidly develops fibrosis in non-alcoholic steatohepatitis. Int J Exp Pathol 94:93–103

Mazzali M, Kipari T, Ophascharoensuk V, Wesson JA, Johnson R, Hughes J (2002) Osteopontin–a molecule for all seasons. Qjm 95: 3–13

Murugaiyan G, Mittal A, Weiner HL (2008) Increased osteopontin expression in dendritic cells amplifies IL-17 production by CD4+ T cells in experimental autoimmune encephalomyelitis and in multiple sclerosis. J Immunol 181:7480–7488

Papatheodoridi AM, Chrysavgis L, Koutsilieris M, Chatzigeorgiou A (2019) The role of senescence in the development of non-alcoholic fatty liver disease and progression to non-alcoholic steatohepatitis. Hepatology (Jun 23). https://doi.org/10.1002/hep.30834

Rangaswami H, Bulbule A, Kundu GC (2006) Osteopontin: role in cell signaling and cancer progression. Trends Cell Biol 16:79–87

Sahai A, Malladi P, Melin-Aldana H, Green RM, Whitington PF (2004) Upregulation of osteopontin expression is involved in the development of nonalcoholic steatohepatitis in a dietary murine model. Am J Physiol Gastrointest Liver Physiol 287:G264–G273

Shinohara ML, Kim JH, Garcia VA, Cantor H (2008) Engagement of the type I interferon receptor on dendritic cells inhibits T helper 17 cell development: role of intracellular osteopontin. Immunity 29:68–78

Syn WK, Choi SS, Liaskou E, Karaca GF, Agboola KM, Oo YH, Mi Z, Pereira TA, Zdanowicz M, Malladi P, Chen Y, Moylan C, Jung Y, Bhattacharya SD, Teaberry V, Omenetti A, Abdelmalek MF, Guy CD, Adams DH, Kuo PC, Michelotti GA, Whitington PF, Diehl AM (2011) Osteopontin is induced by hedgehog pathway activation and promotes fibrosis progression in nonalcoholic steatohepatitis. Hepatology 53:106–115

Syn WK, Oo YH, Pereira TA, Karaca GF, Jung Y, Omenetti A, Witek RP, Choi SS, Guy CD, Fearing CM, Teaberry V, Pereira FE, Adams DH, Diehl AM (2010) Accumulation of natural killer T cells in progressive nonalcoholic fatty liver disease. Hepatology 51:1998–2007

Takahashi A, Kurokawa M, Konno S, Ito K, Kon S, Ashino S, Nishimura T, Uede T, Hizawa N, Huang SK, Nishimura M (2009) Osteopontin is involved in migration of eosinophils in asthma. Clin Exp Allergy 39:1152–1159

Uede T (2011) Osteopontin, intrinsic tissue regulator of intractable inflammatory diseases. Pathol Int 61:265–280

Uede T, Katagiri Y, Iizuka J, Murakami M (1997) Osteopontin, a coordinator of host defense system: a cytokine or an extracellular adhesive protein? Microbiol Immunol 41:641–648

Weber GF (2001) The metastasis gene osteopontin: a candidate target for cancer therapy. Biochim Biophys Acta 1552:61–85

Xanthou G, Alissafi T, Semitekolou M, Simoes DC, Economidou E, Gaga M, Lambrecht BN, Lloyd CM, Panoutsakopoulou V (2007) Osteopontin has a crucial role in allergic airway disease through regulation of dendritic cell subsets. Nat Med 13:570–578

Yamamoto N, Sakai F, Kon S, Morimoto J, Kimura C, Yamazaki H, Okazaki I, Seki N, Fujii T, Uede T (2003) Essential role of the cryptic epitope SLAYGLR within osteopontin in a murine model of rheumatoid arthritis. J Clin Invest 112:181–188

Yamamoto N, Nakashima T, Torikai M, Naruse T, Morimoto J, Kon S, Sakai F, Uede T (2007) Successful treatment of collagen-induced arthritis in non-human primates by chimeric anti-osteopontin antibody. Int Immunopharmacol 7:1460–1470

Yokosaki Y, Matsuura N, Sasaki T, Murakami I, Schneider H, Higashiyama S, Saitoh Y, Yamakido M, Taooka Y, Sheppard D (1999) The integrin alpha(9)beta(1) binds to a novel recognition sequence (SVVYGLR) in the thrombin-cleaved amino-terminal fragment of osteopontin. J Biol Chem 274:36328–36334